Superfluid Behavior of Active Suspensions from Diffusive Stretching

S. C. Takatori and J. F. Brady
Division of Chemistry and Chemical Engineering, California Institute of Technology, Pasadena, California 91125, USA

(Received 11 October 2016; published 6 January 2017)

The current understanding is that the non-Newtonian rheology of active matter suspensions is governed by fluid-mediated hydrodynamic interactions associated with active self-propulsion. Here we discover an additional contribution to the suspension shear stress that predicts both thickening and thinning behavior, even when there is no nematic ordering of the microswimmers with the imposed flow. A simple micromechanical model of active Brownian particles in homogeneous shear flow reveals the existence of off-diagonal shear components in the swim stress tensor, which are independent of hydrodynamic interactions and fluid disturbances. Theoretical predictions from our model are consistent with existing experimental measurements of the shear viscosity of active suspensions, but also suggest new behavior not predicted by conventional models.

DOI: 10.1103/PhysRevLett.118.018003

Shear rheology of suspensions containing self-propelled bodies at low Reynolds numbers has been studied intensively during the past several years. Conventional models predict that fluid disturbances induced by active self-propulsion help to "stretch" or "contract" the fluid along the extensional axis of shear, resulting in large deviations in the effective shear viscosity of the suspension relative to that of the embedding medium [1–3]. In this Letter, we demonstrate that intrinsic self-propulsion engenders a "shear swim stress" that affects the rheology of active systems in previously unreported ways. The swim stress is a "diffusive" stress generated by self-propulsion and is distinct from, and in addition to, the hydrodynamic stress resulting from fluid-mediated hydrodynamic interactions.

Earlier [4,5] we derived a direct relationship between the translational diffusivity $\boldsymbol{D}$ and the stress generated by a dilute suspension of particles, $\boldsymbol{\sigma} = -n\zeta\boldsymbol{D}$, where n is the particle number density and ζ is the hydrodynamic drag coefficient. The effective translational diffusivity of a dilute active system is $\boldsymbol{D}^{\text{swim}} = U_0^2\tau_R\boldsymbol{I}/6$ for times $t > \tau_R$, where U_0 and τ_R are the swimming speed and reorientation time of the particle, respectively. This gives directly the unique mechanical swim stress exerted by active particles, $\boldsymbol{\sigma}^{\text{swim}} = -n\zeta\boldsymbol{D}^{\text{swim}} = -n\zeta U_0^2\tau_R\boldsymbol{I}/6$, which has been used to predict the phase behavior of self-assembling active matter [4,6–8]. The swim stress is analogous to the osmotic Brownian stress of passive particles.

In shear flow, particle motion in the flow gradient direction couples to advective drift in the flow direction (Fig. 1), resulting in nonzero off-diagonal components in the long-time particle diffusivity, $D_{xy} \neq 0$. This directly implies the existence of a nonzero shear component in the swim stress tensor, $\sigma_{xy}^{\text{swim}} = -n\zeta D_{xy}^{\text{swim}}$. In this Letter, we discover that $D_{xy}^{\text{swim}} > 0$ for small shear rates, which gives $\sigma_{xy}^{\text{swim}} < 0$ and a decrease in the effective shear viscosity of active suspensions below that of the surrounding solvent for pusher, puller, and neutral-type microswimmers. As shown in Fig. 1, diffusion of active particles along the extensional axis of shear acts to "stretch" the fluid and reduce the effective shear viscosity, analogous to the effect of the hydrodynamic stress generated by pusher microorganisms. Whereas the swim pressure represents the mechanical confinement of diffusing active particles [4], a nonzero shear swim stress represents the mechanical stress required to prevent shear deformation of the suspension.

To motivate this new perspective, we consider a single rigid active particle that swims with a fixed speed U_0 in a direction specified by a body-fixed unit orientation vector $\boldsymbol{q}$, which relaxes with a time scale τ_R due to rotational Brownian motion (see Fig. 1). The particle is immersed in a continuous Newtonian solvent with viscosity η_0. We analyze the dynamics of the particle in steady simple shear

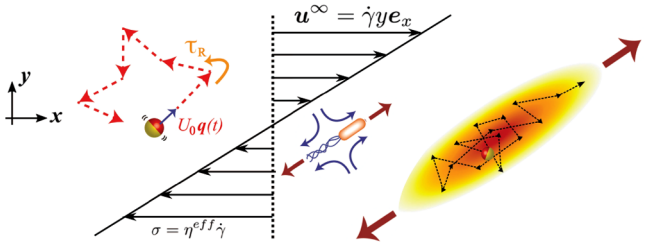

FIG. 1. Schematic of active particles with swimming speed U_0 and reorientation time τ_R in simple shear flow with fluid velocity $u_x^\infty = \dot{\gamma}y$, where $\dot{\gamma}$ is the magnitude of shear rate. The unit vector $\boldsymbol{q}(t)$ specifies the particle's direction of self-propulsion. Diffusion of active particles along the extensional axis of shear acts to "stretch" the fluid and reduce the effective shear viscosity, similar to the effect that the hydrodynamic stress plays for pusher-type microorganisms.

flow $\boldsymbol{u}^\infty = \dot{\gamma} y \boldsymbol{e}_x$, where $\dot{\gamma}$ is the magnitude of shear rate. The Smoluchowski equation governing the probability distribution $P(\boldsymbol{x}, \boldsymbol{q}, t)$ is

$$\frac{\partial P}{\partial t} + \nabla \cdot \boldsymbol{j}_T + \nabla_q \cdot \boldsymbol{j}_R = 0, \tag{1}$$

where the translational and rotational fluxes are given by, respectively [9–11],

$$\boldsymbol{j}_T = (\boldsymbol{u}^\infty + U_0 \boldsymbol{q}) P, \tag{2}$$

$$\boldsymbol{j}_R = \dot{\gamma}(\boldsymbol{q} \cdot \boldsymbol{\Lambda} + B(\boldsymbol{I} - \boldsymbol{qq}) \boldsymbol{q} : \boldsymbol{E}) P - \frac{1}{\tau_R} \nabla_q P. \tag{3}$$

In Eq. (3), the antisymmetric and symmetric velocity-gradient tensors $\boldsymbol{\Lambda}$ and $\boldsymbol{E}$ are nondimensionalized by $\dot{\gamma}$, and $\nabla_q \equiv \partial/\partial \boldsymbol{q}$ is the orientation-space gradient operator. The dynamics of the particle are controlled by a balance between shear-induced particle rotations and the particle's intrinsic reorientation time, given by a shear Péclet number $\mathrm{Pe} \equiv \dot{\gamma}\tau_R$. The constant scalar $B = ((a/b)^2 - 1)/((a/b)^2 + 1)$, where a and b are the semimajor and minor radii of the particle, respectively; $B = 0$ for a spherical particle. The terms in Eq. (2) are the advective contributions from ambient fluid flow and intrinsic self-propulsion of the swimmer. The Stokes-Einstein-Sutherland translational diffusivity, $\boldsymbol{D}_0$, is omitted in Eq. (2), since the magnitude of the self-propulsive contribution $D^{\mathrm{swim}} = U_0^2 \tau_R/6$ may be $\mathcal{O}(10^3)$ larger (or more) than D_0 for many active swimmers of interest.

Following established procedures [5,10,12] (see Supplemental Material [13]), we obtain the steady solution to Eqs. (1)–(3) for times $t > \tau_R$ and $t > \dot{\gamma}^{-1}$ when all orientations have been sampled; the resulting solution gives the effective translational diffusivity, hydrodynamic stress, and swim stress. As shown in Fig. 2, fluid shear introduces anisotropy and nonzero off-diagonal components in the particle diffusivity. The asymptotic solution at small shear rates is $\boldsymbol{D}^{\mathrm{swim}}/(U_0^2\tau_R/6) = \boldsymbol{I} + \mathrm{Pe}(1+B)\boldsymbol{E}/2 + \mathcal{O}(\mathrm{Pe}^2)$. In the flow direction, D_{xx}^{swim} initially increases with a correction of $\mathcal{O}(\mathrm{Pe}^2)$ due to increased sampling of fluid streamlines in the flow gradient direction, but decreases to zero as $\mathrm{Pe} \to \infty$ because the particle simply spins around with little translational movement. This nonmonotonic behavior was also seen in the dispersion of active particles in an external field [5] and sedimentation of noncentrosymmetric Brownian particles [14]. In the flow gradient direction, D_{yy}^{swim} decreases monotonically with increasing Pe. In the vorticity direction, D_{zz}^{swim} is unaffected by shearing motion and is constant for all Pe.

Most interestingly, the off-diagonal diffusivity D_{xy}^{swim} is nonzero, $\mathcal{O}(\mathrm{Pe})$ for small Pe, nonmonotonic, and negative for intermediate values of Pe. Random diffusion in the gradient direction, D_{yy}^{swim}, allows the particle to traverse across streamlines, which couples to the advective drift in the flow direction to give a nonmonotonic off-diagonal shear diffusivity (see schematic in Fig. 1). In an experiment or computer simulation, calculation of shear-induced diffusivity requires attention because advective drift translates the particles in the flow direction, resulting in Taylor dispersion with mean-squared displacements that do not grow linearly with time [15].

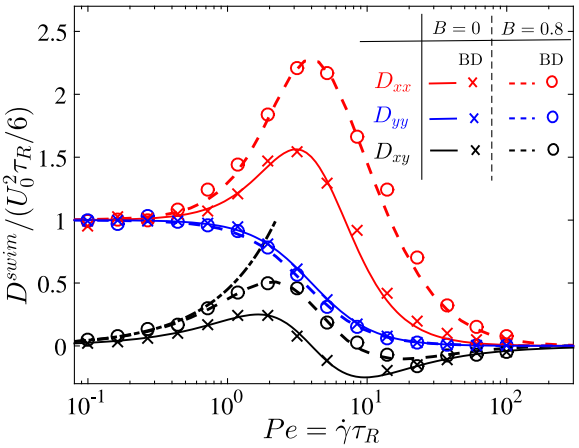

FIG. 2. Swim diffusivity as a function of shear Péclet number for two different values of geometric factor B ($B = 0$ sphere; $B = 0.8$ ellipsoid). Solid and dashed curves are theoretical solutions, and the symbols are Brownian dynamics (BD) simulation results. Dash-dotted curve for D_{xy} is the small-Pe solution for $B = 0.8$.

A nonzero off-diagonal swim diffusivity implies the presence of a shear swim stress from $\sigma_{xy}^{\mathrm{swim}} = -n\zeta D_{xy}^{\mathrm{swim}}$. From Fig. 2 we see that $D_{xy}^{\mathrm{swim}} > 0$ for small Pe, which gives $\sigma_{xy}^{\mathrm{swim}} < 0$ and the effective shear viscosity of the suspension decreases below that of the surrounding solvent. In addition to an indirect calculation of the stress via the diffusivity, we can also compute it directly using the virial expression for the stress. The Langevin equation governing the motion of a single swimmer in simple shear flow (without translational Brownian motion) is $\boldsymbol{0} = -\zeta(\boldsymbol{U} - \boldsymbol{u}^\infty) + \boldsymbol{F}^{\mathrm{swim}}$, where $\boldsymbol{u}^\infty = \dot{\gamma} y \boldsymbol{e}_x$, and $\boldsymbol{F}^{\mathrm{swim}} \equiv \zeta \boldsymbol{U}_0$ is the self-propulsive swim force of the particle [4].

The swim stress is the first moment of the force, $\boldsymbol{\sigma}^{\mathrm{swim}} \equiv -n\langle[\boldsymbol{x}\boldsymbol{F}^{\mathrm{swim}}]^{\mathrm{sym}}\rangle$, where $[\cdot]^{\mathrm{sym}}$ is the symmetric part of the tensor. The angle brackets denote an average over all particle configurations, $\langle(\cdot)\rangle = \int (\cdot) P(\boldsymbol{x}, \boldsymbol{q}) d\boldsymbol{x} d\boldsymbol{q}$, where $P(\boldsymbol{x}, \boldsymbol{q})$ is the steady solution to Eqs. (1)–(3). It is important to ensure symmetry in the swim stress because angular momentum conservation requires the stress to be symmetric in the absence of body couples. Direct calculation of the swim stress via the virial definition (see Supplemental Material [13]) gives results identical to those obtained from the diffusivity-stress relationship; Brownian dynamics simulations also corroborate our result. In our simulations, the particles were evolved following the Langevin equation given above, in addition to the rotational dynamics, $d\boldsymbol{q}/dt = \dot{\gamma}(\boldsymbol{q} \cdot \boldsymbol{\Lambda} + B(\boldsymbol{I} - \boldsymbol{qq})\boldsymbol{q} : \boldsymbol{E}) + \sqrt{2/\tau_R}\boldsymbol{\Gamma}_R \times \boldsymbol{q}$,

where $\boldsymbol{\Gamma}_R$ is a unit random normal deviate: $\overline{\boldsymbol{\Gamma}_R(t)} = \mathbf{0}$ and $\overline{\boldsymbol{\Gamma}_R(t)\boldsymbol{\Gamma}_R(0)} = \delta(t)\boldsymbol{I}$. Results from simulations were averaged over 10^4 independent particle trajectories for times long compared to τ_R and $\dot{\gamma}^{-1}$.

Until this Letter, only the normal components of the swim stress (i.e., $\sigma_{ii}^{\text{swim}}$ where $i = x, y, z$) have been studied [4–8,11,16–24], which give the average pressure required to confine an active body inside of a bounded space. We discover here that the off-diagonal shear swim stress, $\sigma_{xy}^{\text{swim}}$, provides a new physical interpretation of the non-Newtonian shear rheology of active matter.

From continuum mechanics, we have $\nabla \cdot \boldsymbol{\sigma} = \mathbf{0}$ and $\nabla \cdot \boldsymbol{u} = 0$, where $\boldsymbol{\sigma}$ is the total stress of the suspension and $\boldsymbol{u}$ is the suspension-average velocity. The stress can be written as $\boldsymbol{\sigma} = -p_f\boldsymbol{I} + 2\eta_0\dot{\gamma}(1 + 5\phi/2)\boldsymbol{E} + \boldsymbol{\sigma}^{\text{act}}$, where p_f is the fluid pressure, η_0 is the viscosity of the continuous Newtonian solvent, ϕ is the volume fraction of particles ($=4\pi a^3 n/3$ for spheres), $5\phi/2$ is the Einstein shear viscosity correction that is present for all suspensions (taking the result for spherical particles in this Letter), and the active stress is the contribution due to self-propulsion of the particles, $\boldsymbol{\sigma}^{\text{act}} = \boldsymbol{\sigma}^H + \boldsymbol{\sigma}^{\text{swim}}$.

The hydrodynamic stress is $\boldsymbol{\sigma}^H = n\boldsymbol{S}^H = n\sigma_0^H(\langle \boldsymbol{qq}\rangle - \boldsymbol{I}/3)$, where $\boldsymbol{S}^H$ is the hydrodynamic stresslet associated with the swimmers' permanent force dipole, and σ_0^H is its magnitude which scales as $\sigma_0^H \sim \zeta U_0 a$ ($\sigma_0^H < 0$ for "pushers," $\sigma_0^H > 0$ for "pullers") [1,25,26]. For swimmers with an isotropic orientation distribution, $\langle \boldsymbol{qq}\rangle = \boldsymbol{I}/3$, the hydrodynamic stress makes no contribution to the suspension stress. The hydrodynamic stress is present in the model by Saintillan [1] and is the only contribution that has been considered in the literature.

The main contribution of this Letter is the identification and inclusion of an off-diagonal shear component in the swim stress, $\boldsymbol{\sigma}^{\text{swim}} \equiv -n\langle[\boldsymbol{xF}^{\text{swim}}]^{\text{sym}}\rangle$. The swim force of an active Brownian particle is $\boldsymbol{F}^{\text{swim}} \equiv \zeta U_0 \boldsymbol{q}$, so we obtain $\boldsymbol{\sigma}^{\text{swim}} = -n\zeta U_0^2 \tau_R \langle[\bar{\boldsymbol{x}}\boldsymbol{q}]^{\text{sym}}\rangle$, where nondimensional position $\bar{\boldsymbol{x}} = \boldsymbol{x}/(U_0\tau_R)$.

It is important to distinguish and differentiate the swim stress from the hydrodynamic stress. First, $\boldsymbol{\sigma}^{\text{swim}}$ is an entropic term because it arises from the random walk process associated with active swimming and tumbling, whereas $\boldsymbol{\sigma}^H$ comes from fluid-mediated hydrodynamics and the multipole moments generated by self-propulsion. Naturally, this leads to a different scaling of the swim stress $\boldsymbol{\sigma}^{\text{swim}} \sim (n\zeta U_0)(U_0\tau_R)$ compared to the hydrodynamic stress $\boldsymbol{\sigma}^H \sim (n\zeta U_0)a$. The relevant length scale of the swim stress is the swimmer run length, $U_0\tau_R$, as opposed to the hydrodynamic stress that scales with the swimmer size a (see schematic in Fig. 1).

In addition to the two terms above, we know from passive Brownian suspensions that nonspherical particles like polymers and liquid crystals can generate a shear stress from flow-induced particle alignment or stretching [27,28]. Compared with the swim stress, the magnitudes of these terms are $\mathcal{O}[k_BT/(k_sT_s)]$, where $k_sT_s \equiv \zeta U_0^2\tau_R/6$ is the activity scale associated with self-propulsion [6]. For most microswimmers of interest, $k_BT/(k_sT_s) \lesssim \mathcal{O}(10^{-3})$, so these terms are not included in this Letter.

For steady simple shear flow, the shear stress is constant across every plane, and we obtain $\sigma_{xy} = \sigma = \eta^{\text{eff}}\dot{\gamma}$, where the effective viscosity of the suspension is

$$\frac{\eta^{\text{eff}}}{\eta_0} = 1 + \frac{5}{2}\phi + \frac{\sigma_{xy}^H + \sigma_{xy}^{\text{swim}}}{\eta_0\dot{\gamma}}, \tag{4}$$

where $\sigma_{xy}^H = n\sigma_0^H\langle q_x q_y\rangle$ and $\sigma_{xy}^{\text{swim}} = -n(\langle xF_y^{\text{swim}}\rangle + \langle yF_x^{\text{swim}}\rangle)/2$. For the active Brownian particle model with swim force $\boldsymbol{F}^{\text{swim}} \equiv \zeta U_0\boldsymbol{q}$, we obtain $\sigma_{xy}^{\text{swim}} = -n\zeta U_0^2\tau_R(\langle \bar{x}q_y\rangle + \langle \bar{y}q_x\rangle)/2$, where $\bar{x}$ and $\bar{y}$ are nondimensionalized by the run length $U_0\tau_R$.

Active spherical particles that do not establish macroscopic orientational order with the imposed flow do not generate a hydrodynamic stress, $\sigma_{xy}^H = 0$, but can exert a nonzero swim stress, giving, for all Pe (see Supplemental Material [13]),

$$\frac{\eta^{\text{eff}}}{\eta_0} = 1 + \frac{5}{2}\phi - \frac{3\phi}{16}\left(\frac{1}{\text{Pe}_R}\right)^2\left(\frac{1 - (\text{Pe}/4)^2}{[1 + (\text{Pe}/4)^2]^2}\right). \tag{5}$$

The reorientation Péclet number $\text{Pe}_R \equiv a/(U_0\tau_R)$ is a ratio of the particle size a to the swimmer run length $U_0\tau_R$. For small Pe and Pe_R, η^{eff} is smaller than the Newtonian viscosity of the surrounding solvent, η_0. With increasing Pe, η^{eff} increases and becomes larger than η_0, until a maximum is reached at intermediate Pe. As $\text{Pe} \to \infty$, the particles spin around in place without taking a step, so η^{eff} approaches a constant given by the solvent's viscosity plus the Einstein correction. This nonmonotonic behavior has not been predicted previously because conventional models do not include the swim stress.

For nonspherical particles, the hydrodynamic drag tensor varies with the orientation as $\boldsymbol{\zeta} = \zeta_\parallel\boldsymbol{qq} + \zeta_\perp(\boldsymbol{I} - \boldsymbol{qq})$, where $\zeta_\parallel$ and $\zeta_\perp$ are the parallel and perpendicular components, respectively. We assume here that the direction of self-propulsion is aligned with the body-fixed axisymmetric polar axis, $\boldsymbol{U}_0 = U_0\boldsymbol{q}$, so the swim diffusivity-stress relationship becomes $\boldsymbol{\sigma}^{\text{swim}} = -n\zeta_\parallel\boldsymbol{D}^{\text{swim}}$.

Analytical solutions to Eqs. (1)–(3) are not available for nonspherical particles, so a perturbation analysis for small Pe gives the swim stress $\boldsymbol{\sigma}^{\text{swim}}/(n\zeta_\parallel U_0^2\tau_R/6) = -\boldsymbol{I} - \text{Pe}(1 + B)\boldsymbol{E}/2 + \mathcal{O}(\text{Pe}^2)$, and the hydrodynamic stress $\boldsymbol{\sigma}^H/(n\sigma_0^H) = B\text{Pe}\boldsymbol{E}/15 + \mathcal{O}(\text{Pe}^2)$. Substituting these results into Eq. (4), we obtain the effective shear viscosity for small Pe,

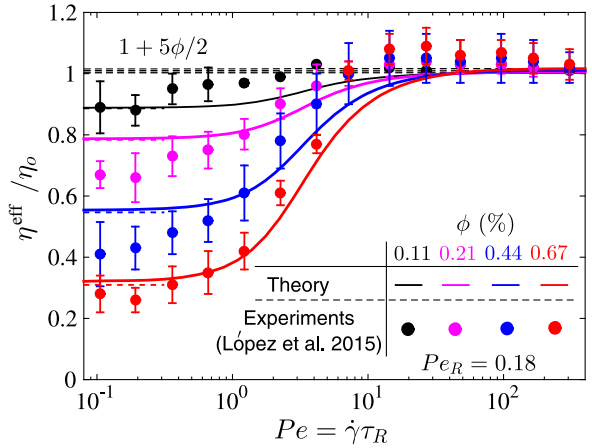

FIG. 3. Comparison of our model, Eq. (4), with shear experiments of López *et al.* [29] with motile *E. coli* bacteria at different concentrations. Horizontal dashed lines for small Pe are the analytical solutions of Eq. (6).

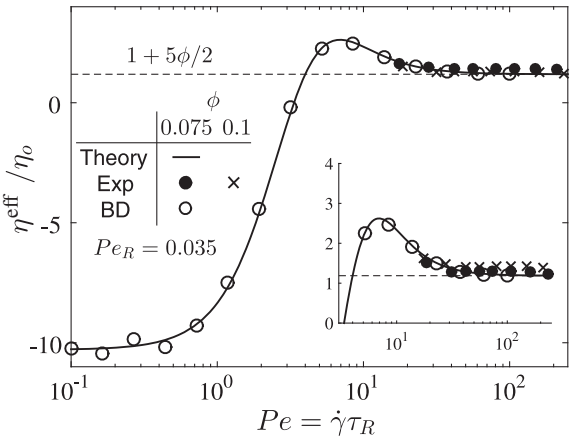

FIG. 4. Effective suspension viscosity of spherical active particles at dilute concentrations and reorientation Péclet number $\mathrm{Pe}_R \equiv a/(U_0\tau_R) = 0.035$. Filled circles and crosses at large Pe are experimental data of Rafaï *et al.* [31] using "puller" microalgae *C. Reinhardtii*. The solid curve is the analytical theory of Eq. (5), and the open circles are BD simulation results. Inset: Magnification at large Pe to show agreement with experiments.

$$\frac{\eta^{\rm eff}(\mathrm{Pe}\to 0)}{\eta_0} = 1+\frac{5}{2}\phi - \left(-\frac{1}{5}B\alpha\mathrm{Pe}_R + \frac{1+B}{4}\right) \times \frac{3\phi}{4\mathrm{Pe}_R^2} K\left(\frac{a}{b}\right), \qquad (6)$$

where α is a parameter associated with the force dipole magnitude, defined as $\alpha \equiv \sigma_0^H/(\zeta_\parallel U_0 a)$, K is the shape factor in the hydrodynamic drag coefficient in the parallel component $\zeta_\parallel = 6\pi\eta_0 bK$, and a and b are the semimajor and minor radii of an ellipsoidal particle, respectively. The constant scalar $B = ((a/b)^2-1)/((a/b)^2+1)$; $B = 0$ for a spherical particle.

Figure 3 compares the effective shear viscosity from our micromechanical model [Eq. (4)] with the experiments of López *et al.* [29]. Physical properties of the *E. coli* bacteria used in our model were taken from their work [29], with swimming speed $U_0 = 20\ \mu$m/s, reorientation time $\tau_R = 4.8$ s, body length $2a = 1.7\ \mu$m, and body diameter $2b = 0.5\ \mu$m, which give the hydrodynamic drag shape factor $K = 1.5$ and geometric coefficient $B = 0.88$. Particle reorientations are modeled in Eq. (3) as a diffusive Brownian process using the run-and-tumble equivalence [30], so τ_R is consistent with that reported by López *et al.* [29], which is a directional persistence time based on the bacteria tumble frequency, $1/\omega = \tau_R/2 = 2.4$ s. The reorientation Péclet number based on the swimmer body length a yields negative effective shear viscosity predictions, so we have adopted the length scale associated with the force dipole strength of the *E. coli*, $l_d = 17.7\ \mu$m from Lopez *et al.* [29], which gives $\mathrm{Pe}_R = l_d/(U_0\tau_R) \approx 0.18$. The force dipole parameter $\alpha \equiv \sigma_0^H/(\zeta_\parallel U_0 a) \approx -15$, which is based on the reported force dipole strength of the bacteria [29], $\sigma_0^H = -3.8 \pm 1.0 \times 10^{-18}$ Pa · m^3.

In the results of Fig. 3, the ratio $\sigma_{xy}^{\rm swim}/(\sigma_{xy}^{\rm swim}+\sigma_{xy}^H) \approx 0.5$ for small Pe and all bacteria concentrations, which quantifies the importance of the swim stress. For swimmers with $\mathrm{Pe}_R \ll 1$ such as puller microalgae *C. Reinhardtii*, the hydrodynamic stress plays a negligibly small role and the swim stress dominates. Figure 4 compares our model with the experimental data of Rafaï *et al.* [31], who measured the effective shear viscosity of a suspension containing *C. Reinhardtii*. Physical properties of the microalgae used in our model were taken from their work [31], with swimming speed $U_0 = 40\ \mu$m/s, reorientation time $\tau_R = 3.5$ s, and body radius $a = 5\ \mu$m, giving $\mathrm{Pe}_R \equiv a/(U_0\tau_R) \approx 0.035$. This motile microorganism has a spherical body but can align with an imposed flow, perhaps due to rheotaxis or small asymmetry arising from the two flagella used for self-propulsion. The solid curve in Fig. 4 is the analytical theory of Eq. (5) which does not involve the hydrodynamic stress. We obtain good agreement with experimental data and Brownian dynamics simulations, which demonstrates the importance of the shear swim stress for active systems with small reorientation Péclet numbers.

The results in Fig. 4 suggest new behavior not predicted by conventional models. Previous studies [1–3,29] have predicted that puller-type microorganisms like *C. Reinhardtii* increase the effective suspension viscosity above that of the suspending fluid because the hydrodynamic stress is positive for pullers, $\sigma_0^H > 0$. However, the swim stress predicts both thickening and thinning behavior, an increase and decrease of the effective viscosity, for pushers, pullers, and even particles that generate no hydrodynamic stress. Shear thickening and thinning are seen for small Pe_R; they are also present in Fig. 3 but the magnitudes are too small to see. Because the swim stress is large in magnitude compared to the hydrodynamic stress for systems with $\mathrm{Pe}_R \ll 1$, the effective shear viscosity

decreases below η_0 at small shear rates regardless of the swimmer shape or hydrodynamic stress. Further experiments with puller microorganisms at small shear rates are needed to verify if the effective viscosity decreases below the solvent viscosity.

In Fig. 4, we observe a "negative" effective shear viscosity for small Pe, which means that a shear stress must be applied in a direction opposing the flow to maintain a fixed shear rate. The spontaneous onset of active diffusion of particles along the extensional axis of shear can result in a negative effective shear viscosity, analogous to that of active nematics for "pusher" swimmers (see Fig. 1). For a constant shear stress experiment, a reduction in effective viscosity would trigger the shear rate to increase, so a self-regulating processes would preclude a negative viscosity. For active suspensions with a larger concentration of particles, we must include an additional stress contribution from interparticle interactions between the swimmers, $\boldsymbol{\sigma}^P = -n\langle \boldsymbol{x}_{ij}\boldsymbol{F}^P_{ij}\rangle$. Our simulations reveal that the interparticle stress has a negligible effect for the dilute concentrations studied in this Letter. The force moment for the interparticle stress scales as the particle size, so its contribution is $\mathcal{O}(\mathrm{Pe}_R)$ smaller than the swim stress.

S. C. T. is supported by a Gates Millennium Scholars fellowship and a National Science Foundation (NSF) Graduate Research Fellowship (Grant No. DGE-1144469). This work is also supported by NSF Grant No. CBET 1437570.

[1] D. Saintillan, Exp. Mech. **50**, 1275 (2010).
[2] M. C. Marchetti, J. F. Joanny, S. Ramaswamy, T. B. Liverpool, J. Prost, M. Rao, and R. A. Simha, Rev. Mod. Phys. **85**, 1143 (2013).
[3] Y. Hatwalne, S. Ramaswamy, M. Rao, and R. A. Simha, Phys. Rev. Lett. **92**, 118101 (2004).
[4] S. C. Takatori, W. Yan, and J. F. Brady, Phys. Rev. Lett. **113**, 028103 (2014).
[5] S. C. Takatori and J. F. Brady, Soft Matter **10**, 9433 (2014).
[6] S. C. Takatori and J. F. Brady, Phys. Rev. E **91**, 032117 (2015).
[7] S. C. Takatori and J. F. Brady, Soft Matter **11**, 7920 (2015).
[8] S. C. Takatori and J. F. Brady, Curr. Opin. Colloid Interface Sci. **21**, 24 (2016).
[9] M. A. Bees, N. A. Hill, and T. J. Pedley, J. Math. Biol. **36**, 269 (1998).
[10] A. Manela and I. Frankel, J. Fluid Mech. **490**, 99 (2003).
[11] W. Yan and J. F. Brady, J. Fluid Mech. **785**, R1 (2015).
[12] R. N. Zia and J. F. Brady, J. Fluid Mech. **658**, 188 (2010).
[13] See Supplemental Material at http://link.aps.org/supplemental/10.1103/PhysRevLett.118.018003 for analytical calculation of the swim diffusivity and the swim stress via the virial expression for the stress tensor.
[14] Y. Almog and I. Frankel, J. Colloid Interface Sci. **157**, 60 (1993).
[15] A. Sierou and J. F. Brady, J. Fluid Mech. **506**, 285 (2004).
[16] S. C. Takatori, R. De Dier, J. Vermant, and J. F. Brady, Nat. Commun. **7**, 10694 (2016).
[17] W. Yan and J. F. Brady, Soft Matter **11**, 6235 (2015).
[18] X. Yang, M. L. Manning, and M. C. Marchetti, Soft Matter **10**, 6477 (2014).
[19] S. A. Mallory, A. Šarić, C. Valeriani, and A. Cacciuto, Phys. Rev. E **89**, 052303 (2014).
[20] B. Ezhilan, R. Alonso-Matilla, and D. Saintillan, J. Fluid Mech. **781**, R4 (2015).
[21] A. P. Solon, J. Stenhammar, R. Wittkowski, M. Kardar, Y. Kafri, M. E. Cates, and J. Tailleur, Phys. Rev. Lett. **114**, 198301 (2015).
[22] R. G. Winkler, A. Wysocki, and G. Gompper, Soft Matter **11**, 6680 (2015).
[23] R. G. Winkler, Soft Matter **12**, 3737 (2016).
[24] F. Smallenburg and H. Löwen, Phys. Rev. E **92**, 032304 (2015).
[25] D. Saintillan and M. J. Shelley, Phys. Fluids **20**, 123304 (2008).
[26] D. Saintillan and M. J. Shelley, Phys. Rev. Lett. **100**, 178103 (2008).
[27] E. J. Hinch and L. G. Leal, J. Fluid Mech. **76**, 187 (1976).
[28] C.-C. Huang, R. G. Winkler, G. Sutmann, and G. Gompper, Macromolecules **43**, 10107 (2010).
[29] H. M. López, J. Gachelin, C. Douarche, H. Auradou, and E. Clément, Phys. Rev. Lett. **115**, 028301 (2015).
[30] M. E. Cates and J. Tailleur, Europhys. Lett. **101**, 20010 (2013).
[31] S. Rafaï, L. Jibuti, and P. Peyla, Phys. Rev. Lett. **104**, 098102 (2010).